Electronic Supplementary Information (ESI)

Site-selective occupation, optical spectra regulation and photoluminescence properties investigation of Eu^{2+}-activated blue light-excited yellow-orange emitting phosphors

Wenzhi Sun [a, *], Tingting Zhao [a], Shuya Wang [a], Denghu Wei [b], Mengmeng Jiao [c] and Hongwu Zhang [a, *]

[a] School of Chemistry and Materials Science, Ludong University, Yantai 264025, P. R. China.

[b] School of Materials Science and Engineering, Liaocheng University, Liaocheng 252059, P. R. China.

[c] School of Physics and Optoelectronic Engineering, Ludong University, Yantai 264025, P. R. China.

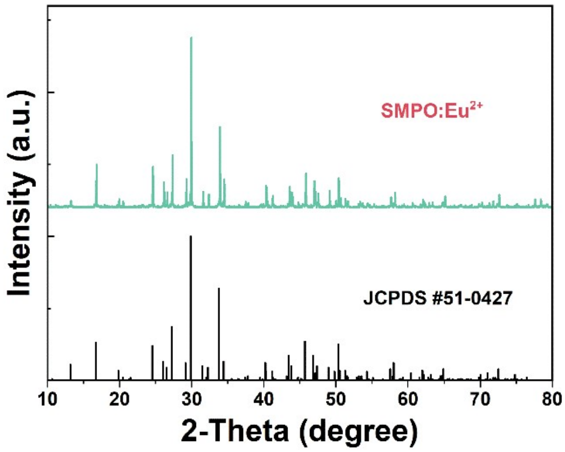

Fig. S1 XRD pattern of SMPO:Eu^{2+} with the standard data $Sr_9Fe_{1.5}(PO_4)_7$.

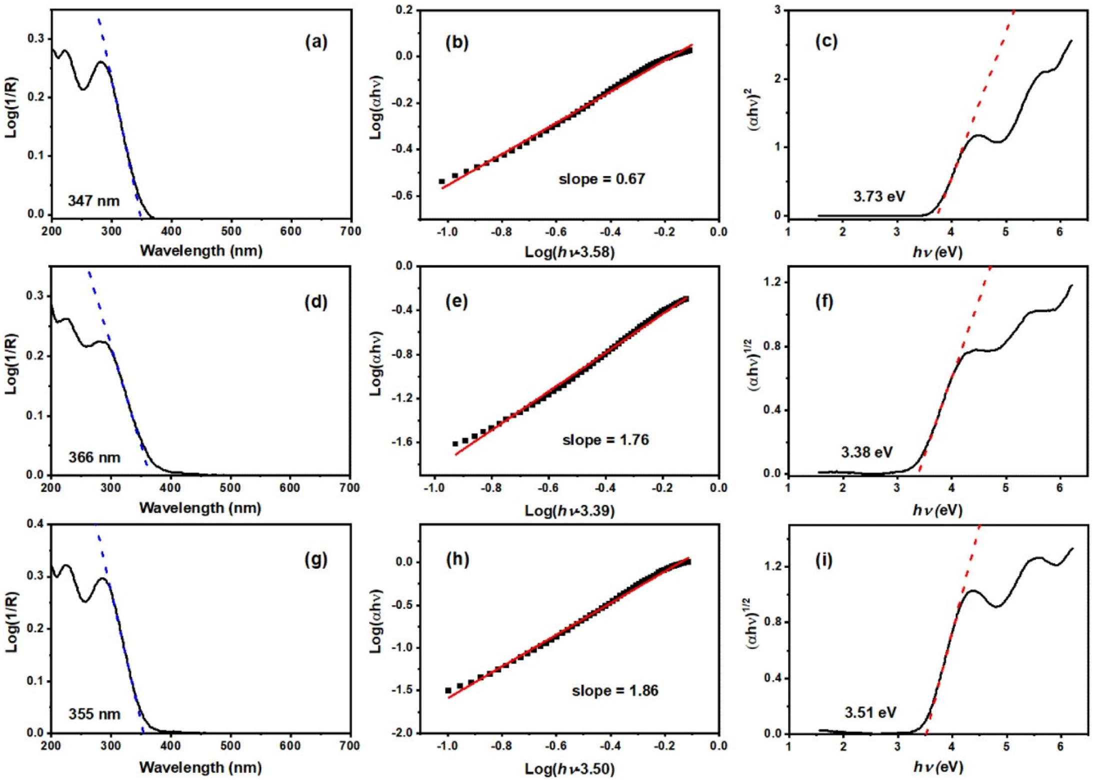

Fig. S2 Determination for the band gaps of (a) $SC_{2.5}MPO$, (b) $SB_{2.5}MPO$ and (c) SMPO. The bandgap can be calculated with the equation: $\alpha h\nu = A(h\nu - E_g)^{n/2}$ [1]. This equation can be derived as: $Log(\alpha h\nu) = (n/2) \times Log(h\nu - E_g) + LogA$. n = 1 and 4 indicates direct bandgap and indirect bandgap, respectively. DRS are transformed to similar forms to absorption spectra. E_g is estimated approximately to be 3.58 eV, 3.39 eV and 3.50 eV for $SC_{2.5}MPO$,

$SB_{2.5}MPO$ and SMPO, respectively, as shown in Fig. S2a, S2d and S2g. Then, $Log(\alpha h\nu)$ *vs.* $Log(h\nu - E_g)$ plots are fitted with liner equation to determine the value of *n*. As shown in Fig. S2b, S2e and S2h, *n* is calculated to be 1 for $SC_{2.5}MPO$, and 4 for $SB_{2.5}MPO$ and SMPO. Therefore, $SC_{2.5}MPO$ has direct bandgap, and $SB_{2.5}MPO$ and SMPO have indirect bandgaps. Hence, $(\alpha h\nu)^2$ *vs.* $h\nu$ is plotted in Fig. S2c; while $(\alpha h\nu)^{1/2}$ *vs.* $h\nu$ are plotted in Fig. S2f and Fig. S2i. The bandgaps are determined by the straight line to $h\nu$ axis: 3.73 eV, 3.38 eV and 3.51 eV for $SC_{2.5}MPO$, $SB_{2.5}MPO$ and SMPO, respectively.

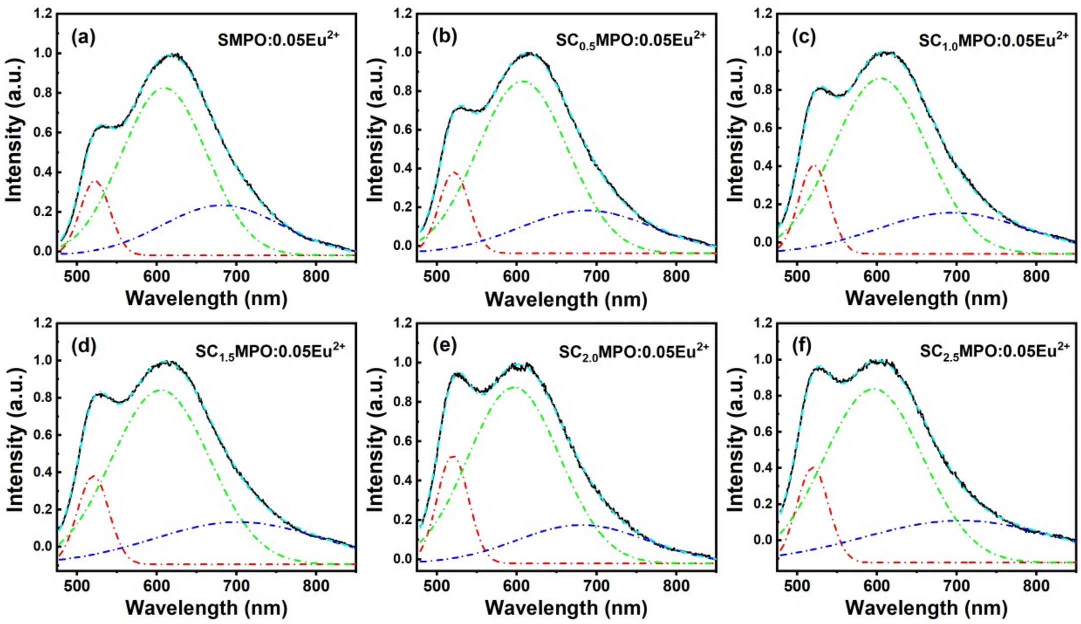

Fig. S3 (a–f) PL spectra and Gaussian fitted curves of $SC_xMPO:Eu^{2+}$ (x = 0–2.5) excited at 460 nm

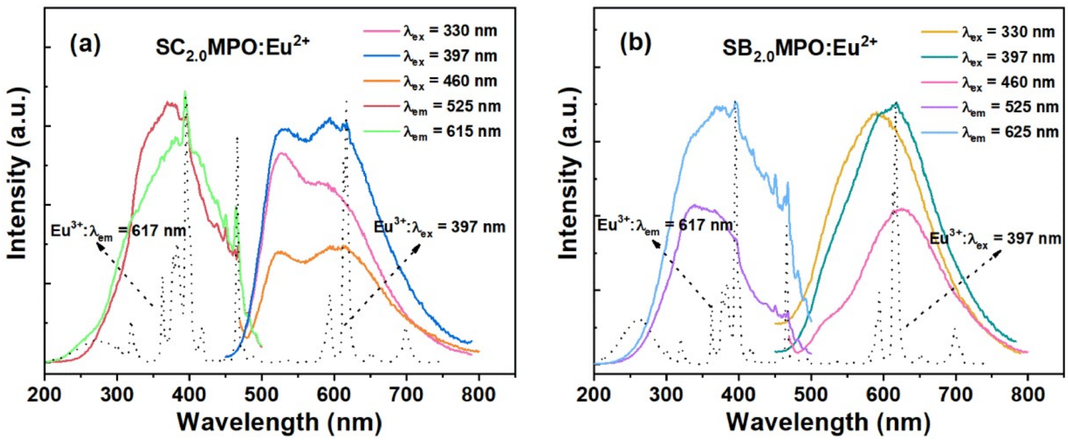

Fig. S4 (a) PLE and PL spectra of $SC_{2.0}MPO:Eu^{2+}$ (solid lines) and normalized $SC_{2.0}MPO:Eu^{3+}$ (dotted lines); (b) PLE and PL spectra of $SB_{2.0}MPO:Eu^{2+}$ (solid lines) and normalized $SB_{2.0}MPO:Eu^{3+}$ (dotted lines)

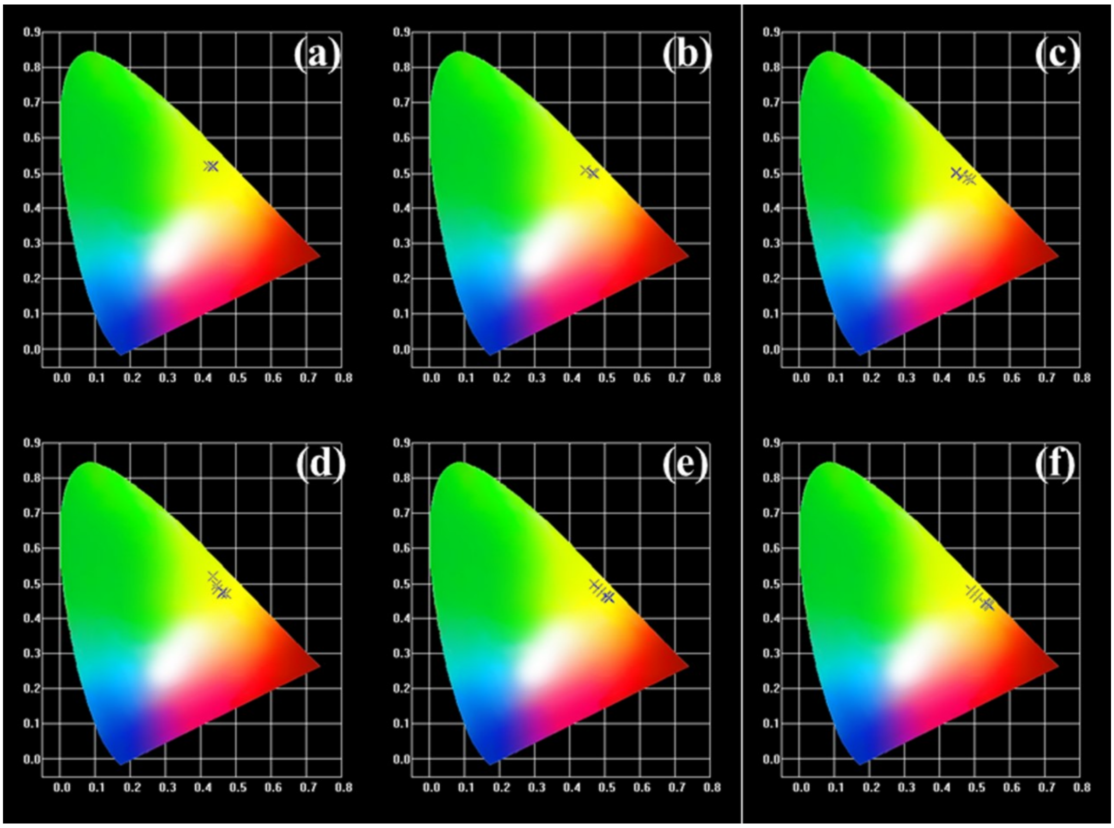

Fig. S5 CIE chromaticity diagram of $SC_xMPO:Eu^{2+}$ (x = 0–2.5) under the excitation of (a) 330 nm, (b) 397 nm and (c) 400 nm; CIE chromaticity diagram of $SB_yMPO:Eu^{2+}$ (y = 0–3.0) under the excitation of (d) 330 nm, (e) 397 nm and (f) 400 nm.

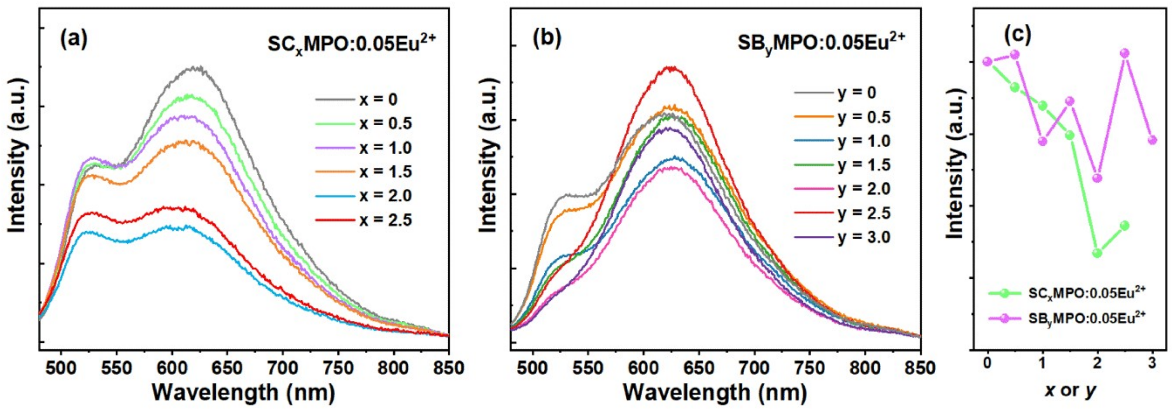

Fig. S6 PL spectra of (a) $SC_xMPO:Eu^{2+}$ (x = 0–2.5) and (b) $SB_yMPO:Eu^{2+}$ (y = 0–3.0); (c) PL intensity of $SC_xMPO:Eu^{2+}$ and $SB_yMPO:Eu^{2+}$ (λ_{ex} = 460 nm)

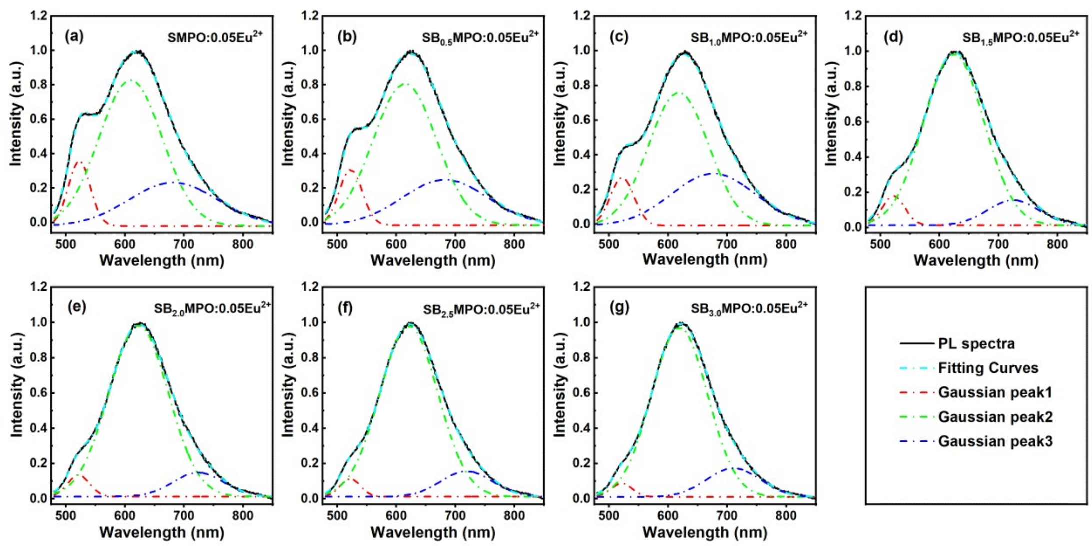

Fig. S7 (a–g) PL spectra and Gaussian fitted curves of $SB_yMPO:Eu^{2+}$ (y = 0–3.0) excited at 460 nm

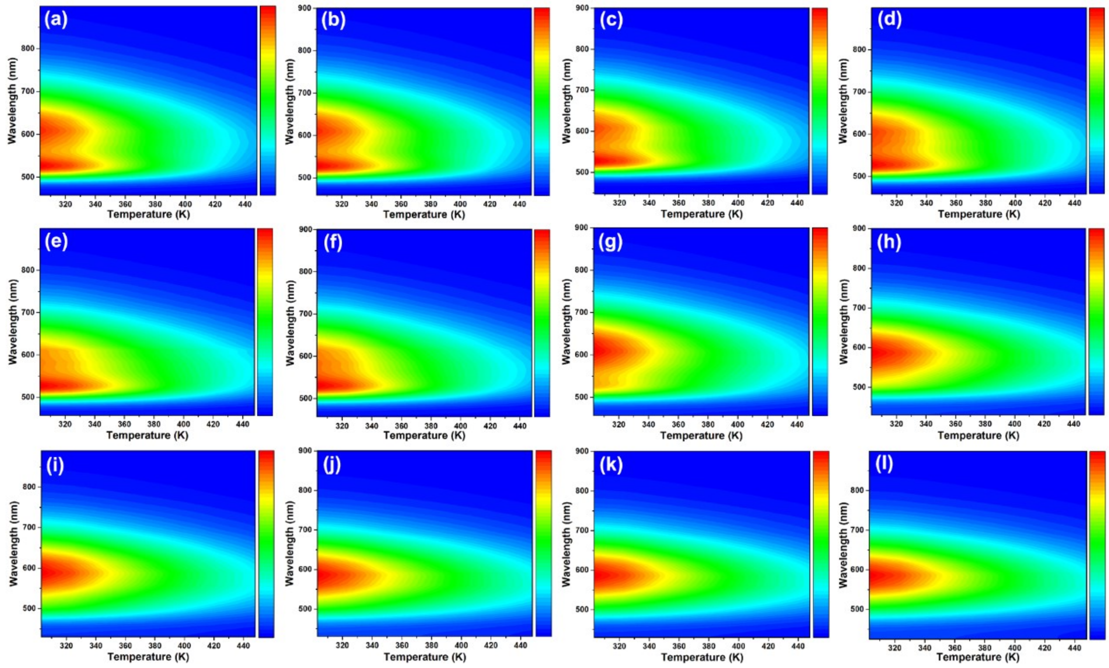

Fig. S8 PL spectra of (a–f) $SC_xMPO:Eu^{2+}$ (x = 0–2.5) and (g–l) $SB_yMPO:Eu^{2+}$ (y = 0.5–3.0) with various temperatures (T = 300–448 K)

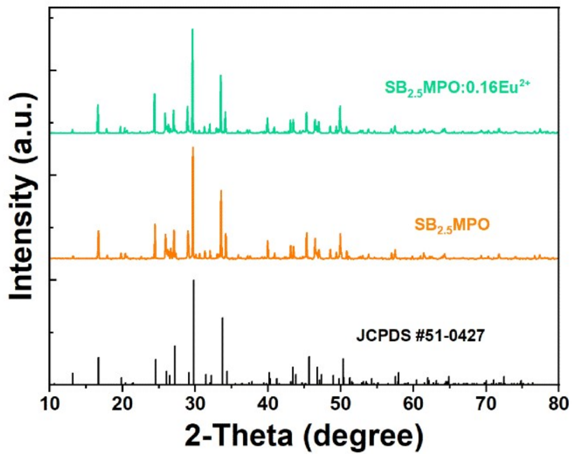

Fig. S9 XRD patterns of $SB_{2.5}MPO:zEu^{2+}$ (z = 0 and 0.16) with the standard data $Sr_9Fe_{1.5}(PO_4)_7$

Table S1 Ionic radii (Å) of Sr^{2+}, Ca^{2+}, Ba^{2+}, Fe^{2+}, Mg^{2+} and Eu^{2+} under different CNs and D_r values

	CN = 6	CN = 7	CN = 8	CN = 9
Sr^{2+}	1.18	1.21	1.26	1.31
Ca^{2+}	1.0	1.06	1.12	1.18
Ba^{2+}	1.35	1.38	1.42	1.47
Fe^{2+}	0.78	--	0.92	--
Mg^{2+}	0.72	--	0.89	--
Eu^{2+}	1.17	1.20	1.25	1.30
D_r(Mg-Fe)	7.7%	--	3.3%	--
D_r(Ca-Sr)	15.3%	12.4%	11.1%	9.9%
D_r(Ba-Sr)	-14.4%	-14.1%	-12.7%	-12.2%
D_r(Eu-Sr)	0.85%	0.83%	0.79%	0.76%

Table S2 CIE coordinates of SC_xMPO:Eu^{2+} (x = 0–2.5) and SB_yMPO:Eu^{2+} (y = 0.5–3.0) under different excitation wavelengths

CIE coordinates (x, y)	λ_{ex} = 330 nm	λ_{ex} = 397 nm	λ_{ex} = 400 nm	λ_{ex} = 460 nm
SMPO:Eu^{2+}	(0.434 0.520)	(0.465, 0.500)	(0.469, 0.497)	(0.491, 0.479)
$SC_{0.5}$MPO:Eu^{2+}	(0.433, 0.521)	(0.460, 0.503)	(0.464, 0.500)	(0.479, 0.486)
$SC_{1.0}$MPO:Eu^{2+}	(0.432, 0.521)	(0.455, 0.505)	(0.458, 0.503)	(0.468, 0.493)
$SC_{1.5}$MPO:Eu^{2+}	(0.434, 0.517)	(0.454, 0.504)	(0.457, 0.502)	(0.466, 0.494)

$SC_{2.0}MPO:Eu^{2+}$	(0.422, 0.520)	(0.446, 0.506)	(0.445, 0.507)	(0.447, 0.500)
$SC_{2.5}MPO:Eu^{2+}$	(0.423, 0.519)	(0.441, 0.509)	(0.444, 0.507)	(0.447, 0.502)
$SB_{0.5}MPO:Eu^{2+}$	(0.444, 0.495)	(0.477, 0.487)	(0.481, 0.485)	(0.501, 0.470)
$SB_{1.0}MPO:Eu^{2+}$	(0.448, 0.482)	(0.485, 0.476)	(0.489, 0.475)	(0.510, 0.459)
$SB_{1.5}MPO:Eu^{2+}$	(0.463, 0.474)	(0.499, 0.467)	(0.503, 0.466)	(0.529, 0.446)
$SB_{2.0}MPO:Eu^{2+}$	(0.459, 0.471)	(0.501, 0.464)	(0.504, 0.463)	(0.532, 0.442)
$SB_{2.5}MPO:Eu^{2+}$	(0.472, 0.469)	(0.509, 0.462)	(0.512, 0.460)	(0.540, 0.440)
$SB_{3.0}MPO:Eu^{2+}$	(0.466, 0.467)	(0.508, 0.459)	(0.512, 0.458)	(0.543, 0.436)

Table S3 Parameters of the fabricated LED devices

	Device 1	Device 3
R1	80.86	96.11
R2	88.42	90.23
R3	95.04	83.60
R4	74.34	79.90
R5	78.44	91.27
R6	86.21	87.63
R7	85.67	80.80
R8	68.68	83.97
R9	23.66	90.21
R10	74.57	78.91
R11	72.26	85.63

R12	60.88	73.97
R13	82.03	93.97
R14	97.20	90.94
R15	72.17	90.96

*Note: The luminous efficiency of Device 3 is 40.61 lm/W.

Reference

1. L. Zhang, D. Wang, Z. Hao, X. Zhang, G.-h. Pan, H. Wu and J. Zhang, *Adv. Opt. Mater.*, 2019, **7**, 1900185.